

Analysis of test results under static load conditions of 316L steel

Grzegorz Szala¹, Karolina Karolewska^{1,*} and Mateusz Wirwicki¹

¹UTP University of Science and Technology in Bydgoszcz, Faculty of Mechanical Engineering, al. Prof. S. Kaliskiego 7, 85-796 Bydgoszcz, Poland

Abstract. Metal powder 3D printing technology is gaining popularity due to the possibility of producing structural elements of complex geometry, which production with the methods used so far is difficult or impossible to obtain. An example of a material used in the parts production by the additive method is 316L steel, which is used in the production of bone support screws, surgical tools and needles, or in other industries for the production of exhaust manifolds, parts of furnaces or heat exchangers. The study investigated the mechanical properties, hardness and microstructure of 316L steel produced in the selective laser melting process (SLM). Based on the tests, the following mechanical properties of 316L steel were obtained: $S_u = 566.7\text{MPa}$, $S_{p0.2} = 484\text{MPa}$, $E = 113820\text{MPa}$, $A = 79.5\%$, $Z = 72.3\%$. The hardness test results show a significant increase in hardness as the tensile test approaches the sample fracture. The structure of 316L steel in the grip part is characterized by the formation of visible semi-elliptical zones of the material alloy, the pools with crystallized grains with a cell-column structure oriented in the direction of the thermal gradient. This type of microstructure is characteristic of technology in which, after solidification, the cooling process takes place at high speed.

1 Introduction

Additive technologies are used to produce objects with complex geometry that cannot be achieved with traditional machining methods. Selective laser melting is one of the additive manufacturing methods, which consists in melting the applied powder thread until the finished element is formed in accordance with the 3D model. Due to the possibility of making an element of any shape, additive technologies have started to be used in many industries: medicine, aviation, and automotive [1]. In the field of medicine, incremental manufacturing is used to produce bone implants, e.g. made of Ti6Al4V alloy, Ti6Al4V alloy [2,3] and zirconium oxide [4] dental implants, screws supporting fractured bones and elements to supplement their deficiencies, prosthetic and orthopedic elements, needles for surgical or pacemaker electrodes made of 316L steel. Moreover, 316L steel, due to its properties, is used in the construction of exhaust manifolds, parts of furnaces, heat exchangers, parts of jet engines, etc. [5, 6]. The study [7] investigated the tensile properties of elements made of 316L stainless steel used, inter alia, in the aviation industry. It was found that the SLM process parameters should be optimized for different alloys and this should be carefully considered at the design stage. It has been observed that the mechanical properties of the SLM parts are strongly dependent on the laser energy density that was used to manufacture the parts. It was found that the tensile strength and yield point increased when the laser energy density was increased to 62.5 J/mm^3 for 316L, while the elongation decreased. This article [8] presents the results of studies on the influence of print orientation and scanning angle on the mechanical properties of 316L stainless steel. The tensile strength S_u is significantly

* Corresponding author: karolina.karolewska@utp.edu.pl

influenced by the print density. Manufacturing errors (spheroidization, shrinkage and incomplete fusion) can cause changes in the weakest zone and affect the direction of the crack. To improve the mechanical properties of 316L steel, heat treatments are used to affect the microstructural, mechanical and corrosive properties of 316L stainless steel produced by SLM selective laser melting. The longer heat treatment time reduces the hardness of the steel. The strength of 316L steel was lower after heat treatment due to the reduction of dislocation density, while better plasticity (approx. 40-50%) was obtained after full annealing [6].

The aim of the work is to determine the static properties of 316L steel made with the additive method, and to analyze the hardness and microstructure test results.

The scope of the work covers the presentation of the mechanical properties of 316L steel (i.e. tensile strength R_m , yield strength $R_{p0.2}$, elongation A , contraction Z and Young's modulus E), analysis of the hardness distribution and microstructure of the material.

2 Material and test specimen

The sample for testing under static load conditions was made of 316L steel. This material is characterized by a low carbon content, which translates into good mechanical properties, good machinability and resistance to oxidation and corrosion.

Table 1. Chemical composition of 316L steel according to ASTM F3184.

| Alloying element | Content in % |
|------------------|--------------|
| Cr | 16.0÷18.0 |
| Ni | 10.0÷14.0 |
| Mo | 2.0÷3.0 |
| Mg | ≤ 2.0 |
| Si | ≤ 1.0 |
| N | ≤ 0.1 |
| O | ≤ 0.1 |
| P | ≤ 0.045 |
| C | ≤ 0.03 |
| S | ≤ 0.03 |
| Fe | balance |

The mechanical properties of steel strongly depend on their microstructure, which is influenced by phase changes, precipitation and recrystallization. In the case of austenitic stainless steels, heat treatment does not have a significant effect on the hardness and strength, because the reinforcement depends mainly on the characteristics of the phase transformations of the steel, especially austenite-martensite. Table 1 shows the chemical composition of 316L steel in relation to the ASTM F3184 standard.

The research objects were made with the additive technology of selective laser melting - SLM. The test objects were printed on the ProX DMP 320 device with the dimensions of the working platform 275 mm x 275 mm x 420 mm. The thickness of the applied layer was 30 μm , while the spot size was 60 μm . During printing, the laser power was variable, adjusted to the layer, and its maximum value was 500 W. The printing direction of the sample was

consistent with the Z axis. The geometry of steel specimen and their physical form are shown in Figure 1.

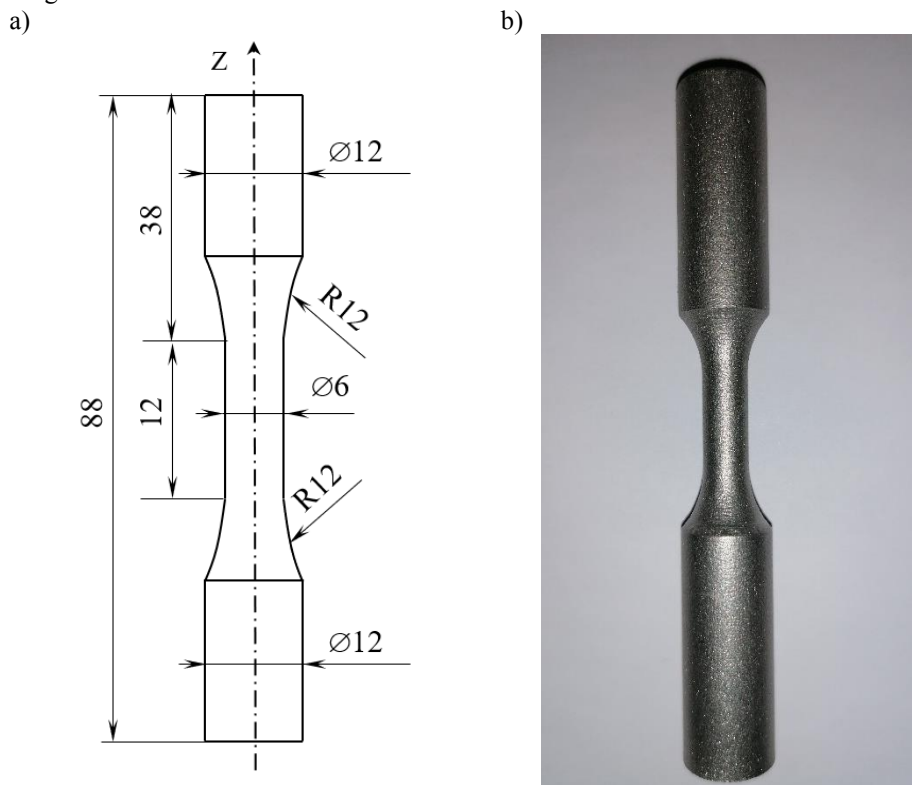


Fig. 1. The specimen for testing under static load conditions: a) geometric features, b) physical form.

3 Test results

3.1 Test results under static load conditions

In order to determine the static properties of the material (tensile strength R_m , yield strength $R_{p0.2}$, elongation A , Young's modulus E), a static tensile test was carried out in accordance with the recommendations of PN-EN ISO 6892-1: 2016. The controlling parameter during the tests was the displacement of the machine piston, which was 0.05 mm / s. During the tests, the loading force and deformation were recorded. The tests were carried out with the use of an extensometer with a measuring base of 10 mm and a measuring range of 1 mm. Table 2 and Figure 2 show the test results for 316L steel.

Table 2. Mechanical properties of 316L steel.

| | Su | Sy0.2 | E | A | Z |
|-----------------|--------|--------|---------------|------|------|
| | MPa | MPa | MPa | % | % |
| Own research | 566.7 | 484 | 113820 | 79.5 | 72.3 |
| ISO 6892-1:2009 | 507±26 | 464±26 | 167000 ±26000 | 40±5 | - |

Comparing the obtained strength values R_m with its normative range, it can be stated that they are higher than $\sim 9.8\%$. The yield point for the 316L material produced by the additive method is within the range specified by the standard. The values of Young's modulus obtained as a result of the tests are significantly lower than those given in ISO 6892-1: 2009. The E-module value for the extensometer is $\sim 31.8\%$ lower. However, the value of the elongation A obtained is about 98.8% higher than that given in the standard.

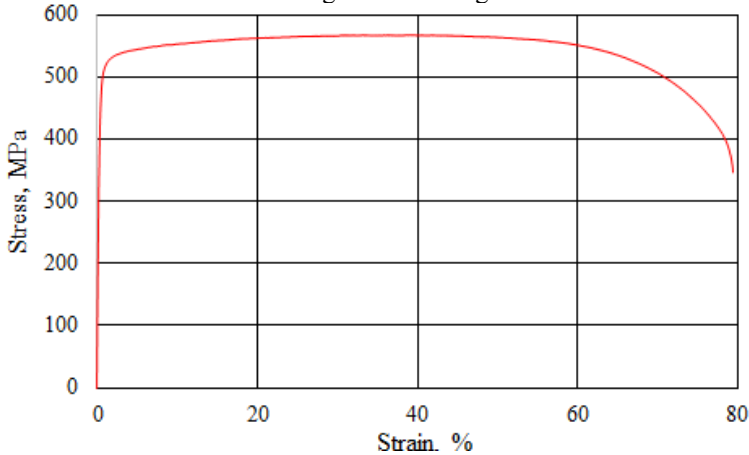


Fig. 2. Tensile diagram for 316L steel obtained as a result of the tests.

3.2 Hardness test results

Material hardness tests were carried out on specimens cut from samples subjected to the static tensile test. 316L steel hardness was measured using the Vickers method. The hardness test stand was the HUATEC HV-10 hardness tester. The test load during the tests was 98.07N, which made it possible to determine the hardness on the HV10 scale. Hardness measurements were made in several planes: along the Z axis (Fig. 3a), on the xy plane in the grip part of the sample (Fig. 3a) and on the xz-I plane in the grip part and xz-II in the measuring part of the sample (Fig. 3b).

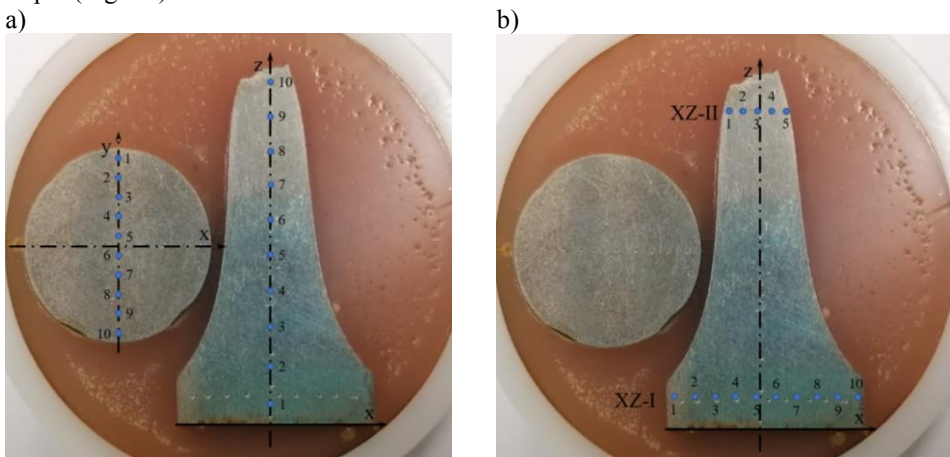


Fig. 3. Measurement points in the hardness test: a) along the Z axis and on the xy plane, b) on the xz plane in the gripping and measuring part.

Table 3. Hardness test results using the Vickers method.

| Measurement point | Measurement plane | | | |
|-------------------|-------------------|-------|-------|-------|
| | Z | XY | XZ-I | XZ-II |
| 1 | 230.5 | 229.5 | 220.0 | 368.0 |
| 2 | 226.5 | 227.0 | 226.0 | 379.5 |
| 3 | 229.0 | 221.0 | 228.0 | 373.0 |
| 4 | 226.0 | 227.0 | 228.5 | 405.5 |
| 5 | 230.0 | 225.5 | 224.5 | 379.5 |
| 6 | 241.5 | 230.5 | 228.5 | |
| 7 | 283.0 | 234.0 | 227.0 | |
| 8 | 320.0 | 232.0 | 227.5 | |
| 9 | 342.0 | 228.0 | 223.5 | |
| 10 | 378.5 | 235.0 | 220.5 | |

Table 3 presents the results of hardness measurements in various planes, while Figure 4 shows the developed graphs of hardness changes for individual planes. The graphs are described with the fourth degree polynomial and the coefficient of determination R^2 .

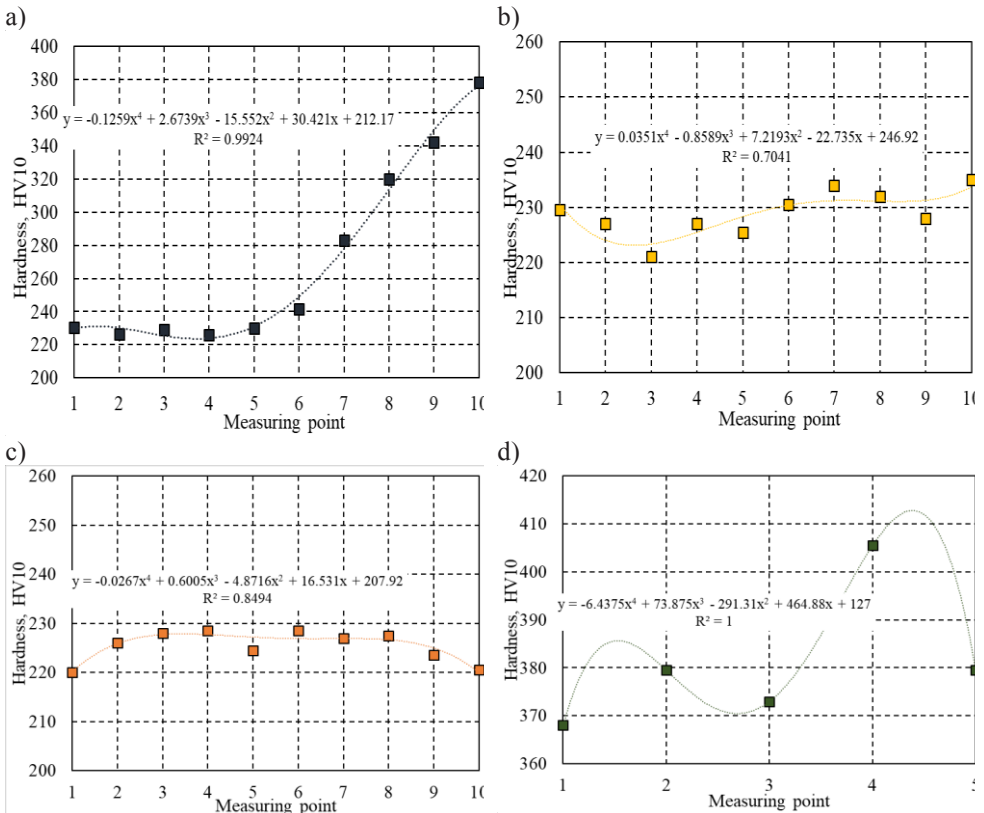


Fig. 4. Hardness distribution charts: a) along the Z axis, b) on the xy plane, c) on the xz-I plane in the gripping part, d) on the xz-II plane in the measuring section.

When analyzing the obtained hardness results, it can be noticed that the measurements taken along the Z axis are characterized by an increase in value with the approach to the sample fracture as a result of the static tensile test. The difference between the lowest hardness value in the gripping part and the highest value in the measuring part is 152.5 HV10. The increase in hardness along the Z axis may be related to changes in the microstructure caused by material deformations as a result of the tensile test. Similar relationships for another material, which is the titanium alloy Ti6Al4V made with additive technology, were obtained in the works [9, 10]. The material hardness on the xy plane ranges from 221.0 ÷ 235.0 HV10, which is a slight difference 14 HV10 hardness in this area. The results obtained on the xy plane reach values comparable to those presented for the xz-I plane in the grip part of the sample. The hardness difference on the xz-I plane is only 8.5 HV10. The highest hardness values were obtained for the xz-II plane in the measuring part, which was subjected to large deformations.

3.3 Microstructure analysis

After the static tensile test was performed, specimens were taken from the test samples in order to make microscopic photos. The microscopic photos were taken in the gripping part and the measuring part of the sample, which is schematically shown in Figure 5a. Figure 5b shows the microstructure in the measuring part, while Figure 5c in the handle part.

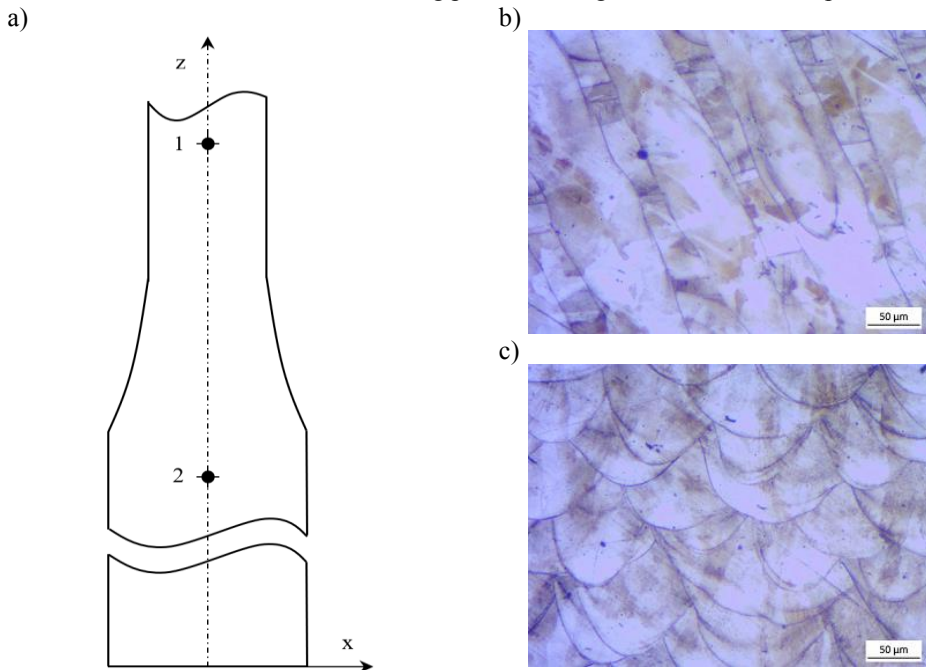


Fig. 5. The 316L steel microstructure: a) a diagram with the places where microstructural photos were taken, b) microstructure in the measuring part of the sample, c) microstructure in the grip part of the sample.

The structure of 316L steel in the grip part is characterized by the formation of visible semi-elliptical zones of the material alloy, the so-called pools with crystallized grains with a cell-column structure oriented in the direction of the thermal gradient. This type of microstructure is characteristic of technology in which the cooling process takes place at high speed after solidification. Comparing the microstructure in the measuring part with that obtained in the gripping part of the tested element, it is possible to notice a change in the shape and elongation of the material melt zones, and thus also the elongation of the grains.

In both cases, pores were also revealed between successive layers of the alloy, which may be associated with incompletely melted powder particles, which may significantly affect the material's strength properties.

4 Conclusions

The presented results of research on the mechanical properties of 316L steel made by selective laser melting show that they differ from the normative properties for the same material, but produced with classical techniques. This allows us to conclude that the manufacturing process significantly affects the properties of the material.

The hardness test results show a significant increase in hardness as the tensile test approaches the sample fracture. This relationship is best seen when analyzing the test results along the Z axis of the sample, as well as on the xz-II plane in the measuring part of the sample. This means the influence of the deformations occurring during the tensile loss on the obtained hardness results. Larger deformations near the fracture of the sample will cause changes in the structure of the material, which will increase the hardness.

Changes due to deformation in the fracture zone of the sample are also noticeable on microscopic photos. As you approach the sample's fracture site, you can see gradual elongation of the grains, which are the longest in the area where the fracture occurs. The change of microstructure due to the deformations occurring during the tensile test affects the hardness of the material.

References

1. Karolewska K., Ligaj B., MATEC Web of Conferences, no. 290 (2019)
2. Wirwicki M., MATEC Web of Conferences, no. 290 (2019)
3. Karolewska K., Ligaj B., AIP Conference Proceedings, no. 2077 (2019)
4. Wirwicki M., Journal of Materials Research and Technology, no. 9 (2020)
5. Salman O.O., Gammer C., Chaubey A.K., Eckert J., Scudino S., Materials Science and Engineering: A, no. 748 (2019)
6. Kong D., Dong C., Ni X., Zhang L., Yao J., Man C., Cheng X., Xiao K., Li X., Journal of Materials Science & Technology, no. 35 (2019)
7. Yakout M., Elbestawi M. A., Veldhuis S. C., Journal of Materials Processing Tech., no. 266 (2019)
8. Zhang Z., Chu B., Wang L., Lu Z., Journal of Alloys and Compounds, no. 791 (2019)
9. Karolewska K., Ligaj B., Boroński D., Materials, no. 13 (2020)
10. Karolewska K., Ligaj B., Wirwicki M., Szala G., Journal of Materials Research and Technology, no. 9 (2020)